

Continuous Lidar Monitoring of Polar Stratospheric Clouds at the South Pole

BY JAMES R. CAMPBELL, ELLSWORTH J. WELTON, AND JAMES D. SPINHIRNE

Polar stratospheric clouds (PSC) play a primary role in the formation of annual “ozone holes” over Antarctica during the austral sunrise. Meridional temperature gradients in the lower stratosphere and upper troposphere, caused by strong radiative cooling, induce a broad dynamic vortex centered near the South Pole that decouples and insulates the winter polar airmass. PSC nucleate and grow as vortex temperatures gradually fall below equilibrium saturation and frost points for ambient sulfate, nitrate, and water vapor concentrations (generally below 197 K). Cloud surfaces promote heterogeneous reactions that convert stable chlorine and bromine-based molecules into photochemically active ones. As spring nears, and the sun reappears and rises, photolysis decomposes these partitioned compounds into individual halogen atoms that react with and catalytically destroy thousands of ozone molecules before they are stochastically neutralized.

Nitrates are most efficient at inhibiting catalytic ozone-destroying cycles. However, their vapor uptake during PSC growth and subsequent particle sedimentation, arising from accompanying increases in fall velocity, cause molecular redistribution to lower levels (i.e., denitrification of the lower stratosphere). Satellite limb-sounder measurements indicate that nitric acid (HNO_3), for example, may be completely removed near

18.0 km above mean sea level (MSL) in air surrounding the South Pole by mid-June each season. In the absence of nitrates, it is only with the overturning of the polar vortex in spring that catalytic processes cease and ozone concentrations are replenished through airmass exchange with the lower latitudes.

Despite a generic understanding of the “ozone hole” paradigm, many key components of the system, such as cloud occurrence, phase, and composition; particle growth mechanisms; and denitrification of the lower stratosphere have yet to be fully resolved. Satellite-based observations have dramatically improved the ability to detect PSC and quantify seasonal polar chemical partitioning. However, coverage directly over the Antarctic plateau is limited by polar-orbiting tracks that rarely exceed 80°S .

Ground-based measurements of PSC can supplement gaps in satellite coverage. Such data are fundamental given that lower-stratospheric temperatures are climatologically coldest there relative to surrounding regions. PSC properties at the South Pole represent those at one end of a longitudinal cross-section of the polar vortex where cloud microphysical and denitrification processes likely vary as a function of thermal and dynamic structure. Furthermore, the meridional mixing of air across the polar vortex boundary from baroclinic disturbances and planetary-scale wave breaking—which incrementally replenishes necessary cloud components during winter diminished by particle growth and fallout (i.e., nitric acid and water vapor)—is negligible nearest the pole. Unfortunately, the deployment of suitable instrumentation atop the Antarctic plateau is limited by accessible infrastructure.

CONTINUOUS PSC MONITORING AT THE SOUTH POLE.

A NASA Micropulse Lidar Network¹ instrument (NASA MPLNET; $0.527\ \mu\text{m}$ in current instruments) was first deployed in December

AFFILIATIONS: CAMPBELL—University Corporation for Atmospheric Research, Visiting Scientist Programs, Naval Research Laboratory, Monterey, California; WELTON—NASA Goddard Space Flight Center, Greenbelt, Maryland; SPINHIRNE—Department of Electrical and Computer Engineering, University of Arizona, Tucson, Arizona

CORRESPONDING AUTHOR: James R. Campbell, c/o Naval Research Laboratory, 7 Grace Hopper Ave., Stop 2, Monterey, CA 93943

E-mail: jamesc@ucar.edu

DOI:10.1175/2008BAMS2754.1

©2009 American Meteorological Society

¹ <http://mplnet.gsfc.nasa.gov>

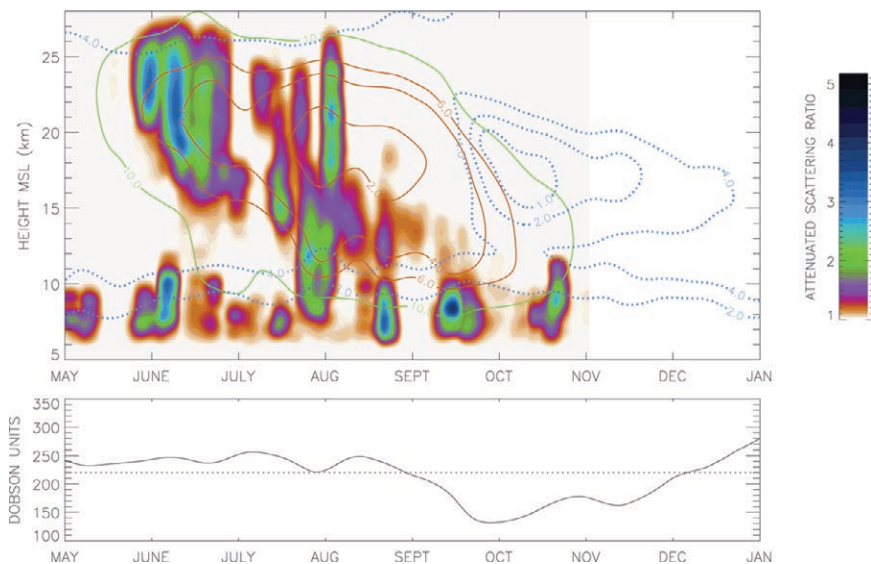


FIG. 1. (top) For May to October 2007, from 5.0 to 28.0 km MSL, composite profiles of smoothed (see text) PSC attenuated scattering ratio (color bar on right), theoretical NAT equilibrium formation isopleths for 10.0-ppbv HNO_3 /4.0-ppmv H_2O concentration (green), and theoretical ice frost-point isopleths for 6.0-, 4.0-, and 2.0-ppmv water vapor concentrations (red). **For May to December 2007, ozone partial pressure isobars are shown for 4.0, 2.0, and 1.0 mPa (blue dashed).** **(bottom)** For May to December 2007, Dobson Unit measurements from 2.85 km MSL, with the dotted line representing 220 DU, or the colloquial threshold for “ozone hole” conditions.

1999 to the NOAA Earth Systems Research Laboratory (NOAA ESRL) Atmospheric Research Observatory (ARO; 89.98°S, 24.80°W, 2.835 km MSL) at the Amundsen–Scott South Pole Station for continuous cloud and aerosol profiling. MPLNET instruments are eye-safe, capable of full-time autonomous operation, and suitably rugged and compact to withstand long-term remote deployment. With only brief interruptions during the winters of 2001 and 2002, a nearly continuous data archive exists to the present.

Shown in Fig. 1 are MPLNET attenuated scattering ratios (ASR; i.e., the relation between attenuated lidar cloud signal and that of the molecular atmosphere, derived as a function of air density) measured from May to October 2007 at the South Pole at 5.0 to 28.0 km MSL. These data were derived using an algorithm optimized for MPLNET retrievals, which relies on the uncertainties of the Level 1.0 processed signal product to detect clouds in low signal-to-noise profiles. PSC are apparent in these data from late May through September above roughly 12.0 km MSL. Below this height, differentiation between stratospheric events and those influenced by upper-tropospheric disturbances, which are apparent throughout the

entire 6-month period at lower levels, is considered ambiguous.

Raw ASR retrievals have been smoothed here to 0.5-day and 0.250-km resolutions using a Hanning function (commonly referred to as the “Von Hann” window) with 5.0-day and 0.750-km temporal and spatial half-width settings. This step removes nearly all of the fine structure typically exhibited with ASR in experimental measurements at standard resolutions. However, it also fills in some gaps where instrument sensitivity may have been briefly limited (i.e., attenuation effects of low-level transmissive clouds). We present these results here for qualitative analysis.

Overlaid on these ASR data in Fig. 1 are corresponding mean equilibrium

saturation isopleths for nitric acid trihydrate (NAT; green) and ice (red) based on ozonesonde temperature profiles collected by NOAA staff scientists onsite (compared with regular daily meteorological balloonsondes, ozonesondes regularly reach 28.0 km MSL in winter before bursting). These data have been smoothed to 1.0-day and 0.050-km temporal and spatial half-widths. Isopleths depict saturation with respect to theoretical background concentrations of 10.0 ppbv HNO_3 and 4.0 ppmv water vapor for NAT (green) and 6.0, 4.0, and 2.0 ppmv water vapor for ice (red), respectively.

For this work, saturation with respect to NAT may be considered a proxy for the presence of the so-called type-I PSCs. The composition and phase of type I PSCs vary as relatively large ($r > 1.0 \mu\text{m}$) frozen nitric acid hydrate solutions (type Ia), small ($r \sim 0.5 \mu\text{m}$) metastable $\text{HNO}_3/\text{H}_2\text{O}$ or ternary ($\text{HNO}_3/\text{H}_2\text{O}/\text{H}_2\text{SO}_4$) solution droplets (type Ib), or small nonspherical particles consisting of metastable $\text{HNO}_3/\text{H}_2\text{O}$ solid phases (type Ic). The presence of water ice, at temperatures below the H_2O frost point, is referred to as type-II PSC. Since temperature is

proportional to saturation vapor pressure, these data may be considered as generalized thermal profiles of the lower stratosphere. Though not direct proxies, these isopleths still reflect the extent and depth of the seasonal cooling.

When considered relative to previous years in the MPLNET PSC database, cloud macrophysical characteristics seen in 2007 match well with mean observations. Clouds were first recorded near 25.0 km MSL in late May and remained persistent through June. This is a very common scenario. Clouds were then episodic near and above 15.0 km MSL in July and August. It is typically during this time period when variability in cloud frequency and their vertical extent is

greatest between seasons. Midseason conditions in 2007 deviated only slightly from the mean, as cloud tops approached 25.0 km MSL (an unusually high level beyond June) on a few occasions in July and early August. This result led to relatively high values of seasonally integrated ASR being derived above 20.0 km MSL. This finding was offset, however, by relatively low totals of seasonally integrated ASR calculated between 12.0 and 20.0 km MSL, which we attribute to relatively few cloud episodes being observed in August and September.

The effects of denitrification and dehumidification in the polar airmass can be seen most clearly in August. At that time, saturation with respect to each of the theoretical vapor concentrations considered was calculated between 15.0 and 20.0 km MSL, amidst the coldest seasonal air. However, few PSC were observed at this time, which indicates low incident nitrate and water vapor concentrations that would otherwise support cloud presence.

Isobars for mean 4.0-, 2.0-, and 1.0-mPa ozone partial pressures are overlaid on the ASR data in Fig. 1 (blue dashed). Column ozone concentrations (in Dobson Units; DU), from ozonesonde datasets

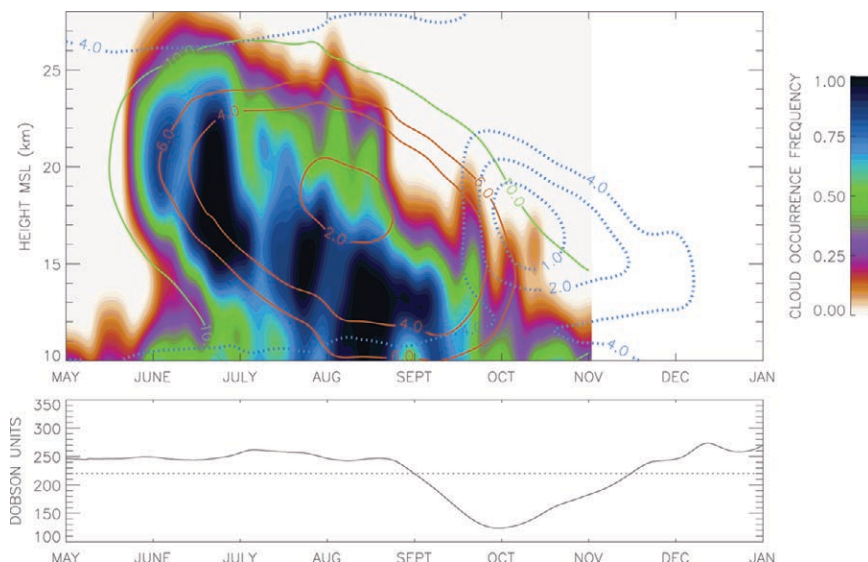


FIG. 2. (top) Stratospheric cloud occurrence frequencies at the South Pole for May to October, from 10.0 to 28.0 km MSL, based on MPLNET datasets from 2000 and 2003–2007. Overlaid are theoretical equilibrium saturation isopleths for nitric acid trihydrate at 10.0 ppbv HNO_3 /4.0 ppmv H_2O , ice at 6.0, 4.0, and 2.0 ppmv H_2O . Ozone partial pressures at 4.0, 2.0, and 1.0 mPa are overlaid from May to December. (bottom) Daily mean measurements of column ozone concentration at 2.85 km MSL for May to December, with the dashed line indicating 220 Dobson Units, which represents the colloquial threshold for “ozone hole” conditions.

smoothed to 1.0-day resolution nearest the surface, are displayed in the lower inset. The dashed line indicates 220 DU, or the colloquial threshold for “ozone hole” conditions. Ozone minima were measured by ozonesondes near and above 15.0 km MSL beginning in early October. Breakup of the polar vortex in 2007, and subsequent overturning of the polar airmass, occurred in December, which was later than the mid-November climatological norm (seen in the lower inset of Fig. 2, and discussed below). This caused ozone-poor air to persist over the area for a longer-than-average period.

SOUTH POLE PSC CLIMATOLOGY (2000, 2003–2007). A 6-year South Pole PSC subset is available through the MPLNET data archive (2000 and 2003–2007). These data are unique, for they lack any significant influence of volcanic aerosols in the lower stratosphere, which may have been present in PSC datasets collected from Antarctica in the 1990s in the aftermath of the 1991 Mt. Pinatubo eruption. Shown in Fig. 2 are cloud occurrence frequencies from 10.0 to 28.0 km MSL for May through October derived from these data.

Once again, we overlay mean equilibrium saturation isopleths for NAT at 10.0 ppbv HNO_3 and 4.0 ppmv water vapor (green) and ice at 6.0, 4.0, and 2.0 ppmv water vapor (red) to approximate saturation states for type-I and type-II PSC in an unperturbed airmass, respectively. Mean ozone partial pressures are again overlaid for 4.0, 2.0, and 1.0 mPa from May through December (blue dashed). Daily 2.85-km MSL measurements of column ozone concentration are shown in the lower inset for May through December, with the 220-DU “ozone hole” threshold denoted.

PSC may be present at the South Pole at any time from late May through early October above 12.0 km MSL. Higher frequencies are observed along a sloping axis centered above 20.0 km MSL in early June and reaching below 15.0 km MSL in mid-August. This closely follows a subsiding core of coldest mean temperatures in the lower stratosphere observed locally each season. Interestingly, the potential for PSC occurring above the 10.0-ppmv NAT saturation isopleth is apparent early in the season. We speculate that, aside from an underestimation of HNO_3 concentration in our calculations, this represents the influence of inertial gravity waves that break in the presence of increased static stability above 25.0 km MSL during the brief period where temperatures are sufficiently cold and HNO_3 concentrations are still relatively unperturbed by the influence of PSC nucleation and settling.

As described above, satellite measurements of denitrification in the airmass surrounding the South Pole indicate a nearly completed process near 18.0 km MSL by mid-June each year. A near-ubiquitous PSC layer is present each season between 18.0 and 25.0 km MSL through June. The redistribution of nitrogen and water vapor, through sublimation and/or evaporation of falling particles, likely enhances the potential for PSC formation below 18.0 km MSL as temperatures gradually become favorable at lower levels over the pole through August. This process may influence the magnitude and spatial depth of eventual ozone losses that are at a maximum locally near and above 15.0 km MSL in October.

Despite extremely cold temperatures, which support saturation for a brief period in late July and early August even at the 2.0-ppmv water vapor frost point, clouds are only episodic from July through September above 15.0 km. These data indicate that cloud occurrence from midseason forward

is likely a function of mixing within the vortex of unperturbed (i.e., nitrate and water vapor-rich) air poleward. In this scenario, isentropic lifting and cooling along poleward trajectories, seen as primary mechanisms for broad-scale cloud formation in recent satellite lidar measurements, would induce PSC that advect over the Antarctic plateau and South Pole.

If confirmed, and our work continues to investigate these data, this process would be expected to convert a greater percentage of available reactive chlorine and bromine within the polar vortex while simultaneously redistributing more nitrogen and water vapor downward. This would lead to greater preconditioning of the polar airmass to catalytic ozone destruction come sunrise. We have, however, found conflicting evidence in our database suggesting that in seasons where circumpolar vortex flow approaches being geostrophic in late July and August (a response to extremely low geopotential heights directly over the pole), meridional transport is inhibited, and the spatial extent of ozone losses outward from the pole actually becomes limited despite unusually cold core temperatures nearest the pole.

CONCLUSIONS AND FUTURE OBJECTIVES. PSC at the South Pole may be considered, in one sense, tracers for the physical and dynamic processes influencing the conditioning of the polar airmass to photolytic/catalytic ozone loss during and after sunrise. Their occurrence near and above 20.0 km MSL in late May and June characterizes an emerging cold core growing radially outward from the dark winter pole. The redistribution of nitrogen and water vapor downward in the lower stratosphere is believed to influence the formation of clouds there in later months as temperatures cool gradually near 15.0 km MSL through August. Episodic clouds observed from July through early October may reflect ageostrophic distortion of the vortex that mixes unperturbed air poleward, where isentropic cooling induces PSC that are then observed over the South Pole. Such a process would introduce a greater component of the polar airmass to heterogeneous chemistry, denitrification, and, eventually, ozone loss.

The colloidal stability of liquid-phase type-I PSC, which form at relatively warm temperatures and low supersaturations, erodes in the presence of solid particle nucleation. Freezing of liquid-phase particles, or the preferential growth of solid particles at the

expense of solution droplets in mixed-phase layers, generate increases to relative fall-velocities in PSC layers. By distinguishing where and when liquid and solid PSC are present, as well as where and when this effective conversion may take place seasonally (given that we know temperatures continue to cool through August at nearly all levels), we would be better positioned to correlate cloud measurements with denitrification and dehumidification processes at the South Pole.

We will seek to expand the MPLNET South Pole experiment for coming years by integrating a depolarization channel into the optical receiver system. This measurement considers the polarization plane of scattered light relative to the linearly polarized transmitted laser source. Spherical particles (i.e., liquid-phase type-I PSC) generate negligible depolarization in contrast to nonspherical ones (i.e., solid-phase type-I and all type-II PSC). Elastic backscatter lidar measurements are not sufficiently robust to accurately characterize composition in these highly complex clouds. Therefore, linear depolarization data would enhance the experiment to its fullest potential for sustained PSC and “ozone hole” climatological studies.

ACKNOWLEDGMENTS. The MPLNET project is funded through the NASA Earth Observing System and the NASA Atmospheric Radiation Sciences program. The authors thank E. G. Dutton and B. Vasel at NOAA ESRL and J. S. Reid at NRL for their continuing support of this work. We also thank E. Hyer, P. Xian at NRL, and the two anonymous reviewers assigned to the manuscript for their comments and insights. Finally, we gratefully acknowledge the work of the many onsite NOAA scientists and technicians at the South Pole who have assisted with both the MPLNET lidar and ozonesonde measurements over the now nine-year experiment.

FOR FURTHER READING

- Campbell, J. R., and K. Sassen, 2008: Polar stratospheric clouds at the South Pole from 5 years of continuous lidar data: Macrophysical, optical and thermodynamic properties. *J. Geophys. Res.*, **113**, D20204, doi:10.1029/2007JD009680.
- , D. L. Hlavka, E. J. Welton, C. J. Flynn, D. D. Turner, J. D. Spinhirne, V. S. Scott, and I. H. Hwang, 2002: Full-time, eye-safe cloud and aerosol lidar observation at Atmospheric Radiation Measurement program sites: Instruments and data processing. *J. Atmos. Oceanic Technol.*, **32**, 439–452.
- , K. Sassen, and E. J. Welton, 2008: Elevated cloud and aerosol layer retrievals from micropulse lidar signal profiles. *J. Atmos. Oceanic Technol.*, **25**, 685–700.
- Gobbi, G. P., G. Di Donfrancesco, and A. Adriani, 1998: Physical properties of stratospheric clouds during the Antarctic winter of 1995. *J. Geophys. Res.*, **103**, 10,859–10,873.
- Palm, S. P., M. Fromm, and J. Spinhirne, 2005: Observations of antarctic polar stratospheric clouds by the Geoscience Laser Altimeter System (GLAS). *Geophys. Res. Lett.*, **32**, L22S04, doi:10.1029/2005GL023524.
- Pfenninger, M., A. Z. Liu, G. C. Papen, and C. S. Gardner, 1999: Gravity wave characteristics in the lower atmosphere at the South Pole. *J. Geophys. Res.*, **104**, 5693–5984, doi:10.1029/98JD02705.
- Shibata, T., K. Sato, H. Kobayashi, M. Yabuki, and M. Shiobara, 2003: Antarctic polar stratospheric clouds under temperature perturbation by nonorographic inertia gravity waves observed by micropulse lidar at Syowa Station. *J. Geophys. Res.*, **108**, 4105, doi:10.1029/2002JD002713.
- Solomon, S., 1999: Stratospheric ozone depletion: A review of concepts and history. *Rev. Geophys.*, **37**, 275–316.
- Tabazadeh, A., M. L. Santee, M. Y. Danilin, H. C. Pumphrey, P. A. Newman, P. J. Hamill, and J. L. Mergenthaler, 2000: Quantifying denitrification and its effect on ozone recovery. *Science*, **288**, 1407–1411.
- , E. J. Jensen, O. B. Toon, K. Drdla, and M. R. Schoeberl, 2001: Role of the stratospheric freezing belt in denitrification. *Science*, **291**, 2591–2594.
- Toon, O. B., A. Tabazadeh, E. V. Browell, and J. Jordan, 2000: Analysis of lidar observations of Arctic polar stratospheric clouds during January 1989. *J. Geophys. Res.*, **105**, 20,589–20,615, doi:10.1029/2000JD900144.
- Waters, J. W., and Coauthors, 2006: The Earth Observing System microwave limb sounder on the Aura satellite. *IEEE Trans. Geosci. Remote Sens.*, **44**, 1075–1092.
- Welton, E. J., J. R. Campbell, J. D. Spinhirne, and V. S. Scott, 2001: Global monitoring of clouds and aerosols using a network of micro-pulse lidar systems. *Proc. Int. Soc. Opt. Eng.*, **4153**, 151–158.